

## Interaction of tin(IV) with doxorubicin ‡

Elisabetta Balestrieri,<sup>a</sup> Linalda Bellugi,<sup>a</sup> Andrea Boicelli,<sup>b</sup> Marcello Giomini,<sup>a</sup>  
Anna Maria Giuliani,<sup>\*,c</sup> Mauro Giustini,<sup>d</sup> Luca Marciari<sup>e</sup> and Peter J. Sadler<sup>\*,†,e</sup>

<sup>a</sup> Dipartimento di Chimica, Università 'La Sapienza', P.le A. Moro 5, 00185 Roma, Italy

<sup>b</sup> CNR, Centro per l'Istochimica, Piazza Botta 10, 27100 Pavia, Italy

<sup>c</sup> Dipartimento di Chimica Inorganica, Via Archirafi 26, 90123 Palermo, Italy

<sup>d</sup> CNR, CS-CFILM, Via Orabona 4, 70126 Bari, Italy

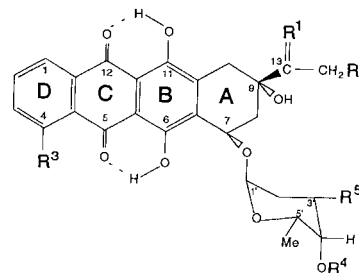
<sup>e</sup> Department of Chemistry, Birkbeck College, University of London, London, UK WC1H 0PP

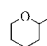
The first study of the interaction of tin(IV) with the anticancer antibiotic doxorubicin in *N,N*-dimethylformamide (dmf) solution is reported. Electronic absorption spectroscopy showed that reaction of the drug with SnCl<sub>4</sub> is time dependent and involves the initial formation of a 1 : 1 complex. The strong binding was also shown by <sup>119</sup>Sn NMR spectroscopy. Reactions with modified anthracyclines show that the  $\alpha$ -ketol side chain at C<sup>9</sup> is essential for interaction, while the quinone chromophore is not involved in binding, as inferred from optical spectroscopy. Proton NMR data suggest that binding to the C<sup>9</sup> side chain involves enolization at C<sup>13</sup>–C<sup>14</sup>. The two-dimensional total correlation spectra indicate that the daunosamine moiety of doxorubicin can be involved in Sn<sup>IV</sup> binding with formation of several time-dependent species. This was verified by <sup>1</sup>H and <sup>119</sup>Sn NMR studies of Sn<sup>IV</sup>–daunosaminide hydrochloride systems. These findings suggest that Sn<sup>IV</sup> can bind to doxorubicin at two sites: the C<sup>9</sup>  $\alpha$ -ketol chain, probably after enolization, and the sugar ring at the 4'-OH and 3'-NH<sub>2</sub> positions. This is the first report of metal binding to doxorubicin at the C<sup>9</sup> side chain.

The clinical use of the anthracycline antibiotic doxorubicin (DX), I, in cancer chemotherapy, although extensive, is limited by its severe negative side effects, the most critical of which is dose-dependent long-term cardiotoxicity, often fatal.<sup>1–6</sup> In addition, drug resistance develops in a number of patients.

Complexation by metal ions<sup>7–19</sup> is one of the many strategies which has been used in attempts to reduce the toxicity of the drug.<sup>20–22</sup> In aqueous solution, it has generally been found that metal ions bind to the C<sup>12</sup>-carbonyl and the C<sup>11</sup>-phenolate oxygens, forming six-membered chelate rings,<sup>7,11,13,15,17</sup> although co-ordination of palladium(II) has been reported to involve also binding to the amino group of daunosamine.<sup>8</sup> Thus, the major binding mode for metal ions involves deprotonation of one phenolic group and formation of a chelating unit resembling the acetylacetonate ligand. This electronic rearrangement is readily detected by electronic absorption spectroscopy, since deprotonation of the phenolic group is accompanied by a decrease in the intensity of the main absorption band centred at 480 nm, paralleled by the appearance of two new bands at 555 and 590 nm, as observed when doxorubicin is deprotonated by titration with a base.<sup>14,23</sup> Tin(IV) compounds themselves are known to exhibit anticancer activity,<sup>24,25</sup> and <sup>119</sup>Sn is an active nucleus for the recently proposed MIRAGE anticancer therapy.<sup>26,27</sup> Association of anthracyclines with Sn<sup>IV</sup> derivatives might therefore prove useful not only to reduce the negative side effects of DX but also possibly to enhance its anticancer potency. As DX binds strongly to DNA,<sup>28</sup> DX might also be used to target this Mössbauer active isotope close to DNA to utilize the resonant absorption of gamma emission by <sup>119</sup>Sn for MIRAGE anticancer therapy.

We have therefore chosen to investigate the interaction of SnCl<sub>4</sub> with DX; the choice of a non-aqueous solvent (*N,N*-dimethylformamide, dmf) has been made to avoid hydrolytic reactions of Sn<sup>IV</sup> which would severely complicate the equilibrium, and also because doxorubicin is soluble enough in



|                    | R <sup>1</sup> | R <sup>2</sup> | R <sup>3</sup> | R <sup>4</sup>  | R <sup>5</sup>               |
|--------------------|----------------|----------------|----------------|---|------------------------------|
| I Doxorubicin      | =O             | OH             | OMe            | H   | NH <sub>3</sub> <sup>+</sup> |
| II Pirarubicin     | =O             | OH             | OMe            |  | NH <sub>3</sub> <sup>+</sup> |
| III Idadoxorubicin | =O             | OH             | H              | H   | NH <sub>3</sub> <sup>+</sup> |
| IV Daunorubicin    | =O             | H              | OMe            | H   | NH <sub>3</sub> <sup>+</sup> |
| V Doxorubicinol    | OH             | OH             | OMe            | H   | NH <sub>3</sub> <sup>+</sup> |
| VI Idarubicin      | =O             | H              | H              | H   | NH <sub>3</sub> <sup>+</sup> |
| VII WP-612         | =O             | OCOMe          | OMe            | H   | OH                           |

this solvent to allow spectral investigations. The data reported here are the first spectroscopic [electronic absorption, circular dichroism (CD), fluorescence and multinuclear NMR] studies on this system.

## Results and Discussion

### DX in dmf

Doxorubicin solutions in dmf, carefully degassed and kept in the dark, are stable for more than 2 d at concentrations in the range 3–16 × 10<sup>-5</sup> M, as shown by the electronic absorption spectrum [Fig. 1(a)] which is unchanged throughout this time. The spectrum closely resembles that observed in aqueous solution at pH < 7 and at concentrations lower than ca. 10<sup>-5</sup> M,<sup>14,23</sup> where DX is essentially monomeric.<sup>23,29</sup> It appears, therefore, that at the concentrations used in the present work in dmf the drug is totally protonated and in the monomeric form, at variance with reports for aqueous solutions at pH 7.4, in which it is

† Present address: Department of Chemistry, The University of Edinburgh King's Building, West Mains Rd., Edinburgh, UK EH9 3JJ.

‡ Based on the presentation given at Dalton Discussion No. 2, 2nd–5th September 1997, University of East Anglia, UK.

**Table 1** Electronic absorption data for doxorubicin in dmf solution ( $r^2$  = correlation coefficient for Beer–Lambert plot)

| $\lambda/\text{nm}$ | $\epsilon/\text{M}^{-1}\text{cm}^{-1}$ | $r^2$  |
|---------------------|--|--------|
| 530                 | 6 210                                  | 0.9997 |
| 496                 | 11 870                                 | 0.9997 |
| 480                 | 12 260                                 | 0.9997 |

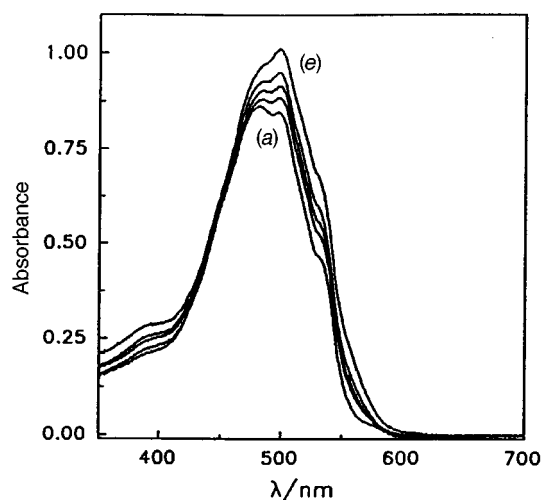


**Fig. 1** The dependence of the electronic absorption spectrum of doxorubicin in dmf on the  $\text{Sn}^{\text{IV}}$ -to-ligand mol ratio,  $R$ . The successive  $R$  values for the spectra from (a) to (e) are: 0, 17, 50, 75, 100.  $[\text{DX}] = 7.8 \times 10^{-5}$  M. Spectra were recorded immediately after mixing. The band is centred at 485 nm, with maxima at 478 and 496 nm, and a shoulder at 530 nm

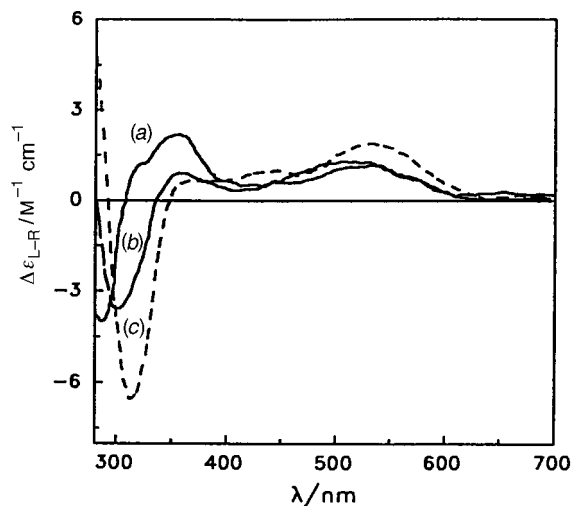


**Fig. 2** The dependence of the circular dichroism spectrum of doxorubicin in dmf on the  $\text{Sn}^{\text{IV}}$ -to-ligand mol ratio,  $R$ . The successive  $R$  values for the spectra from (a) to (c) are: 0, 10, 50.  $[\text{DX}] = 1.6 \times 10^{-4}$  M. Spectra were recorded immediately after mixing. Spectrum (a): positive bands at 360 and 480 nm, negative band at 290 nm; no couplet characteristic of the dimeric associated form (in water: positive band at 460 nm and negative band at 530 nm)

mainly present as a dimer.<sup>23,29</sup> In addition, in the same concentration range, no quenching of fluorescence, typical of dimerization or polymerization processes,<sup>30</sup> was observed, even at the highest concentration, thus confirming the absence of association phenomena. Also the CD spectrum in dmf, in the concentration range  $3.0 \times 10^{-5}$  to  $6.0 \times 10^{-3}$  M, afforded additional evidence for the absence of dimerization, since it exhibited the characteristic pattern of monomeric DX in water.<sup>23,29,30</sup> A typical CD spectrum for a  $1.6 \times 10^{-4}$  M DX solution is presented in Fig. 2(a).

The absorbance of the band centred at 485 nm in the elec-

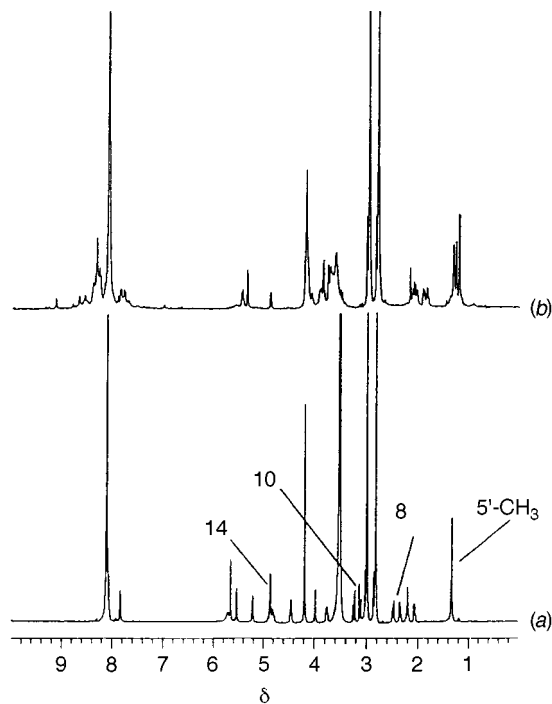


**Fig. 3** Proton NMR spectra of (a) DX alone in  $[\text{2H}_7]\text{dmf}$ , (b) 20 h after the addition of 13 mol equivalents of  $\text{SnCl}_4 \cdot 5\text{H}_2\text{O}$  at 25 °C.  $[\text{DX}] = 3.8 \times 10^{-3}$  M

tronic absorption spectrum follows the Beer–Lambert law, and the molar absorptivities of the three components of the band have been determined and are listed in Table 1.

The one-dimensional proton NMR spectrum of DX in  $[\text{2H}_7]\text{dmf}$  is shown in Fig. 3(a) and the chemical shifts of the aglycone and daunosamine moieties are reported in the Tables 2 and 3, respectively. Peak assignment was made on the basis of the one- and two-dimensional total correlation (TOCSY) spectra and the partial assignments made previously.<sup>31</sup> The spectrum is well resolved, as it is for solvents such as methanol and chloroform, where DX is known to be monomeric, while in aqueous solutions the signals are broadened by auto-aggregation of the drug.<sup>32,33</sup> This behaviour is consistent with the results of CD, fluorescence and electronic absorption spectroscopies. No change was observed in the NMR spectra over a period of 3 d, in agreement with electronic absorption spectroscopic findings.

#### DX– $\text{Sn}^{\text{IV}}$ in dmf

Several systems with tin–doxorubicin molar ratios ranging from 0:1 to 100:1 were studied by electronic absorption spectroscopy. The samples were prepared by mixing separate solutions of  $\text{SnCl}_4$  and DX at appropriate concentrations in a tandem cell.

The addition of  $\text{Sn}^{\text{IV}}$  modified the electronic absorption spectrum of DX and the changes depended on the tin-to-drug mol ratio,  $R$ , as shown in Fig. 1, where spectra are shown for  $R$  values in the range 0:1 to 100:1 for a DX concentration  $7.8 \times 10^{-5}$  M. The modifications become more marked as  $R$  increases. For each value of  $R$ , the spectra are time dependent and a typical set of spectra, for  $R = 50$ , showing the time evolution is presented in Fig. 4, where two clear isosbestic points at 414 and 476 nm, are seen. After evolving for a certain time period, the duration of which depends again on  $R$  and becomes shorter as  $R$  increases (it may vary from 10 h for  $R = 1$  to 80 min for  $R = 100$ ) the spectra remain unchanged for some time (from 50 min at high  $R$  values to 200 min for  $R = 1$ ). Afterwards, further spectral modifications occur and the isosbestic points are lost. A first reactive step can therefore be identified, where only one complex species is in equilibrium with free DX; then,

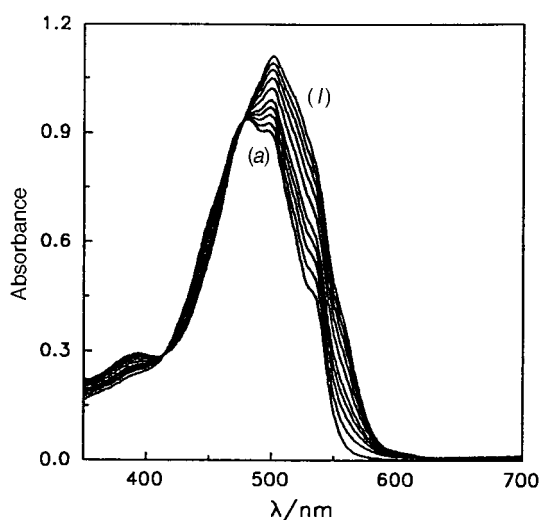
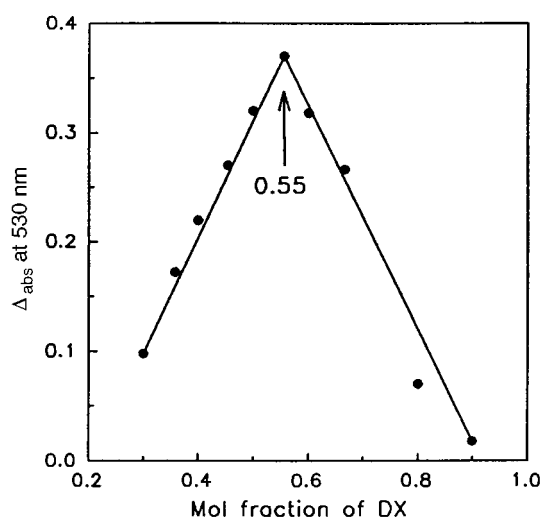
**Table 2** Proton NMR chemical shifts and peak assignments for the aglycone moiety of doxorubicin in  $[^2\text{H}_7]\text{dmf}$  solution ( $T = 25^\circ\text{C}$ ;  $R = 13$ )

| Sample              | $\delta$ (ppm) |      |      |                    |      |                  |                  |                   |                   |                    |
|---------------------|----------------|------|------|--------------------|------|------------------|------------------|-------------------|-------------------|--------------------|
|                     | 1-H            | 2-H  | 3-H  | 4-OCH <sub>3</sub> | 7-H  | 8-H <sub>a</sub> | 8-H <sub>b</sub> | 10-H <sub>a</sub> | 10-H <sub>b</sub> | 14-CH <sub>2</sub> |
| DX                  | 8.05           | 8.08 | 7.83 | 4.19               | 5.21 | 2.35             | 2.49             | 3.13              | 3.25              | 4.86               |
| DX-Sn <sup>IV</sup> | 8.19           | 8.10 | 7.83 | 4.19               | 5.49 | 2.06             | 2.25             | 2.81              | 3.53              | *                  |

\* Not detected.

**Table 3** Proton NMR chemical shifts and peak assignments for the daunosamine moiety of doxorubicin in  $[^2\text{H}_7]\text{dmf}$  solution ( $T = 25^\circ\text{C}$ ;  $R = 13$ )

| Sample              |           | $\delta$ (ppm) |                   |                   |          |                    |          |      |                    |
|---------------------|-----------|----------------|-------------------|-------------------|----------|--------------------|----------|------|--------------------|
|                     |           | 1'-H           | 2'-H <sub>a</sub> | 2'-H <sub>b</sub> | 3'-H     | 3'-NH <sub>2</sub> | 4'-H     | 5'-H | 5'-CH <sub>3</sub> |
| DX                  |           | 5.54           | 2.07              | 2.21              | 3.76     | <i>a</i>           | 3.98     | 4.45 | 1.34               |
| DX-Sn <sup>IV</sup> | Species A | 5.47           | 1.87              | 2.16              | 3.74     | 8.24               | <i>b</i> | 4.09 | 1.35               |
|                     | Species B | 5.37           | 1.96              | 2.13              | 3.94     | 8.32               | <i>b</i> | 3.76 | 1.30               |
|                     | Species C | 4.90           | 1.90              | 2.10              | 3.79     | 8.38               | <i>b</i> | 4.23 | 1.24               |
|                     | Species D | <i>b</i>       | <i>b</i>          | <i>b</i>          | <i>b</i> | <i>b</i>           | <i>b</i> | 4.24 | 1.35               |

<sup>a</sup> NH<sub>3</sub><sup>+</sup>, not detected. <sup>b</sup> Not detected.**Fig. 4** Time dependence of the electronic absorption spectrum of Sn<sup>IV</sup>-DX in dmf at a Sn<sup>IV</sup>-to-ligand mol ratio of 50.  $[\text{DX}] = 7.8 \times 10^{-5}$  M. Spectra (a) to (l) were acquired every 6 min from time zero**Fig. 5** Job's plot for the Sn<sup>IV</sup>-DX system in dmf. Time of equilibration 22 h.  $\Delta_{\text{abs}}$  is the difference of absorbance between systems with doxorubicin mol fraction 1 and *X*

the system evolves leading to other products and more complicated equilibria can be envisioned. Detailed kinetic analyses of this system using electronic absorption spectroscopy are therefore complicated by these factors and cannot be achieved without extensive further work.

Job's plots were obtained by the continuous variation method<sup>34</sup> for Sn<sup>IV</sup>-DX systems at different times of equilibration and a typical plot is shown in Fig. 5 for data obtained at the completion of the first reactive step. The clear-cut maximum occurs for a DX mol fraction of 0.55, indicating a 1:1 stoichiometry for the Sn<sup>IV</sup>-doxorubicin complex formed in this first step. Also the CD spectrum of DX is modified by the interaction with Sn<sup>IV</sup> and again the changes depend on the value of *R* and are time dependent. As shown in Fig. 2 for  $R = 50$ , there are only small changes in the visible region of the spectrum, but a clear shift towards longer wavelength (310 nm) is exhibited by the negative band at 290 nm. This point will be discussed later.

Having established that Sn<sup>IV</sup> can bind to doxorubicin, and forms a 1:1 complex, it is necessary to identify which of the functional groups of the anthracycline are involved in the binding. Previous studies on metal complexes of DX<sup>7,11,13,15,17</sup> suggest that the major site is at C<sup>11</sup>-C<sup>12</sup>, with deprotonation of the phenolic hydroxyl group. Thus, the spectral changes relating to

deprotonation of DX in dmf must first be identified. To achieve this, DX was titrated with a concentrated ethanolic solution of sodium ethoxide and the deprotonation was monitored by electronic absorption and CD spectroscopy. The changes in the electronic absorption spectrum (Fig. 6) are similar to those observed in aqueous solution.<sup>14,23</sup> There is, however, an inversion of the relative intensities of these two maxima on changing the solvent from water to dmf. Deprotonation of DX also modifies the CD spectrum in much the same way as is found in water,<sup>23</sup> and in neither solvent is a shift of the 290 nm band to longer wavelength observed.

The spectral changes accompanying the interaction of DX with Sn<sup>IV</sup>, on the other hand, are totally different and much less conspicuous (Fig. 1): the fine structure of the 485 band in the electronic absorption spectrum is lost, the shoulder at 530 nm increases and a new one grows at 580 nm. A similar loss of resolution is observed on dimerization of DX in aqueous solutions.<sup>35</sup> These observations lead to the conclusion that the tin-drug interaction does not involve the phenolic groups. This deduction is supported by the experiment shown in Fig. 7, where spectrum (a) has been obtained at the end of the first reactive step for a sample with  $R = 1$ . Spectra (b) and (c) have been recorded after addition of an excess of sodium ethoxide and retitration with concentrated hydrochloric acid, respect-

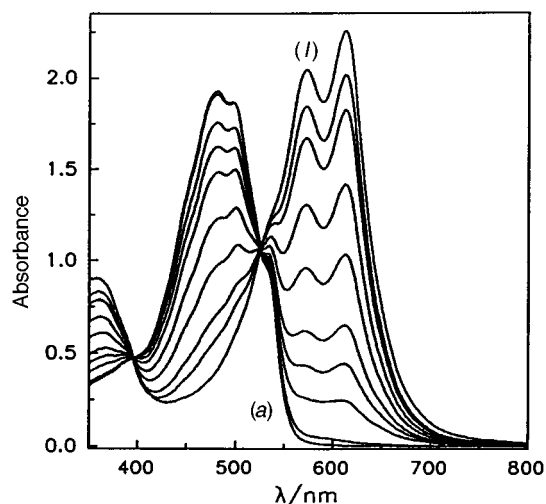


**Fig. 6** Titration of DX in dmf solution with sodium ethoxide.  $[DX] = 1.6 \times 10^{-4}$  M. The amount of added EtONa increases from (a) to (l) (from 0 to 4 mol equivalents). The broad decreasing band is centred at 485 nm, the two growing bands are at 572 and 612 nm (550 and 590, respectively, in water<sup>14,23</sup>)

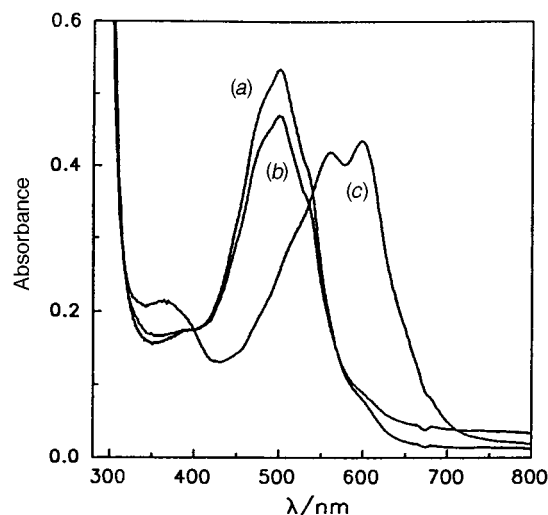


**Fig. 7** Deprotonation of  $\text{Sn}^{\text{IV}}$ -DX in dmf by EtONa and re-titration with HCl. (a)  $\text{Sn}^{\text{IV}}$ -to-ligand mol ratio,  $R = 1$ , at the end of the first reactive step (see text); (b) after the deprotonation of the phenolic group by addition of an excess of EtONa; (c) after re-titration with concentrated HCl. The decrease in intensity of (c) compared to (a) can be accounted for by dilution effects

ively. Deprotonation of the phenolic group is reversible, while the modifications due to complexation with  $\text{Sn}^{\text{IV}}$  are not. At the end of the re-titration the initial spectrum (a) is reproduced, and the full intensity is recovered.

To identify the binding site(s) for  $\text{Sn}^{\text{IV}}$  on DX other than at  $\text{C}^{11}$ - $\text{C}^{12}$ , several anthracyclines modified either in the aglycone or in the sugar moiety and a few simpler model molecules were investigated for their reactivity towards  $\text{Sn}^{\text{IV}}$  in dmf by CD and electronic absorption spectroscopy. The observation of spectral changes similar to those seen with DX were taken as an indication of an interaction of the same type. The results are collected in Table 4, where a plus sign indicates presence of an interaction and a minus sign its absence. All (and only) the compounds which have the  $-\text{CO}-\text{CH}_2\text{OH}$  chain at  $\text{C}^9$  give rise to spectral changes, suggesting that this fragment is essential for the interaction with tin, while the anthraquinone fragment does not seem to be involved.

Binding of  $\text{Sn}^{\text{IV}}$  to doxorubicin is clearly evident from  $^{119}\text{Sn}$  NMR experiments. The spectrum of a  $\text{Sn}^{\text{IV}}$ -DX solution in  $[\text{D}_7\text{H}_7]\text{dmf}$  with  $R = 1$  exhibits two resonances, at  $\delta -339$  and  $-367$ , as compared to the single peak at  $\delta -312$

**Table 4** Detection of CD and electronic absorption spectral changes on reaction of anthracyclines and model compounds with  $\text{Sn}^{\text{IV}}$  in dmf solution

| Compound                           | $\text{C}^9$ $\alpha$ -ketol chain | Spectral changes |
|------------------------------------|------------------------------------|------------------|
| <b>I</b> Doxorubicin               | +                                  | +                |
| <b>II</b> Pirarubicin              | +                                  | +                |
| <b>III</b> Idadoxorubicin          | +                                  | +                |
| Doxorubicinone <sup>a</sup>        | +                                  | +                |
| 7-Deoxydoxorubicinone <sup>a</sup> | +                                  | +                |
| <b>IV</b> Daunorubicin             | -                                  | -                |
| Daunorubicinone <sup>b</sup>       | -                                  | -                |
| <b>V</b> Doxorubicinol             | -                                  | -                |
| <b>VI</b> Idarubicin               | -                                  | -                |
| <b>VII</b> WP-612                  | -                                  | -                |
| Quinizarin                         | -                                  | -                |

<sup>a</sup> Aglycone of **I**. <sup>b</sup> Aglycone of **IV**.

observed for a solution of  $\text{SnCl}_4 \cdot 5\text{H}_2\text{O}$  in  $[\text{D}_7\text{H}_7]\text{dmf}$  at the same concentration.

Proton NMR experiments provided further evidence for the nature of the  $\text{Sn}^{\text{IV}}$  binding sites. These were performed on  $\text{Sn}^{\text{IV}}$ -doxorubicin solutions in  $[\text{D}_7\text{H}_7]\text{dmf}$  with  $R = 1, 2$  or  $13$ . Over a period of 20 h, the spectra exhibited progressive changes, which became more evident as  $R$  increased. The one-dimensional spectrum of a solution with  $R = 13$ , acquired 20 h after mixing, is shown in Fig. 3(b); the peak assignments, obtained *via* a two-dimensional TOCSY experiment, are collected in Tables 2 and 3. The major changes observed in the one-dimensional spectrum were the disappearance of the  $14\text{-CH}_2$  signal and the marked shifts of the  $8\text{-H}_{\text{a,b}}$  and  $10\text{-H}_{\text{a,b}}$  multiplets for the aglycone moiety, while, for the daunosamine moiety, the  $5'\text{-CH}_3$  and  $5'\text{-H}$  resonances were affected: the initial  $5'\text{-CH}_3$  doublet [labelled A in Fig. 8(a)] at  $\delta 1.34$  decreased in intensity and two further doublets at  $\delta 1.30$  and  $1.24$  appeared [labelled B and C, respectively, in Fig. 8(a)]. In the two-dimensional TOCSY spectrum, a total of three new  $5'\text{-CH}_3$ - $5'\text{-H}$  cross-peaks are observed [labelled B, C and D in Fig. 8(b)] and the corresponding  $5'\text{-H}$  resonances are found at  $\delta 3.74, 4.23$  and  $4.24$ , respectively, considerably shifted relative to the initial single quartet at  $\delta 4.09$  [labelled A in Fig. 8(b)]. Except for the  $5'\text{-H}$  and  $-\text{CH}_3$  peaks, the other resonances of the daunosamine moiety of species D could not be assigned, due to spectral overlap and low concentration of this species. It was detectable only through its  $5'\text{-H}$ - $5'\text{-CH}_3$  cross-peak. Different sets of cross-peaks connectivity patterns were found for other daunosamine protons as well. Their signals were shifted, as reported in Table 3; it was not possible to assign the chemical shifts for the  $4'\text{-H}$  resonances, due to overlap.

New sets of cross-peaks were found in the TOCSY spectrum around  $\delta 8.3$ , with connectivities to the  $2'\text{-H}$  and  $3'\text{-H}$  resonances. The clear through-bond connectivities with  $2'\text{-H}_{\text{a}}$ ,  $2'\text{-H}_{\text{b}}$  and  $3'\text{-H}$  suggested assignment to the  $3'\text{-NH}_2$  protons of a  $\text{Sn}^{\text{IV}}$ -daunosamine product; a proton is probably displaced by  $\text{Sn}^{\text{IV}}$  from the  $\text{NH}_3^+$  group at the  $3'$  position even in the initial species A, because we could detect the  $3'\text{-NH}_2$  signal for this species as well.

We also followed the time evolution of  $5'\text{-CH}_3$  peaks A, B and C by acquiring  $^1\text{H}$  NMR one-dimensional spectra every 25 min (Fig. 9). The data suggest the presence of two reaction phases: during the first 5 h the populations of the intermediates B and C increase and subsequently decrease, while the amount of the initial species A is continuously decreasing with time. At longer times, other products, like species D, not detected in the one-dimensional NMR spectrum, would form, though degradation of DX should not be neglected.<sup>36-38</sup>

A  $^1\text{H}$  NMR study of  $\text{Sn}^{\text{IV}}$  binding to the daunosamine moiety was carried out using methyl- $\beta$ -L-daunosaminide hydrochloride (DA) and 1 or 13 mol equivalents of  $\text{SnCl}_4$ , in

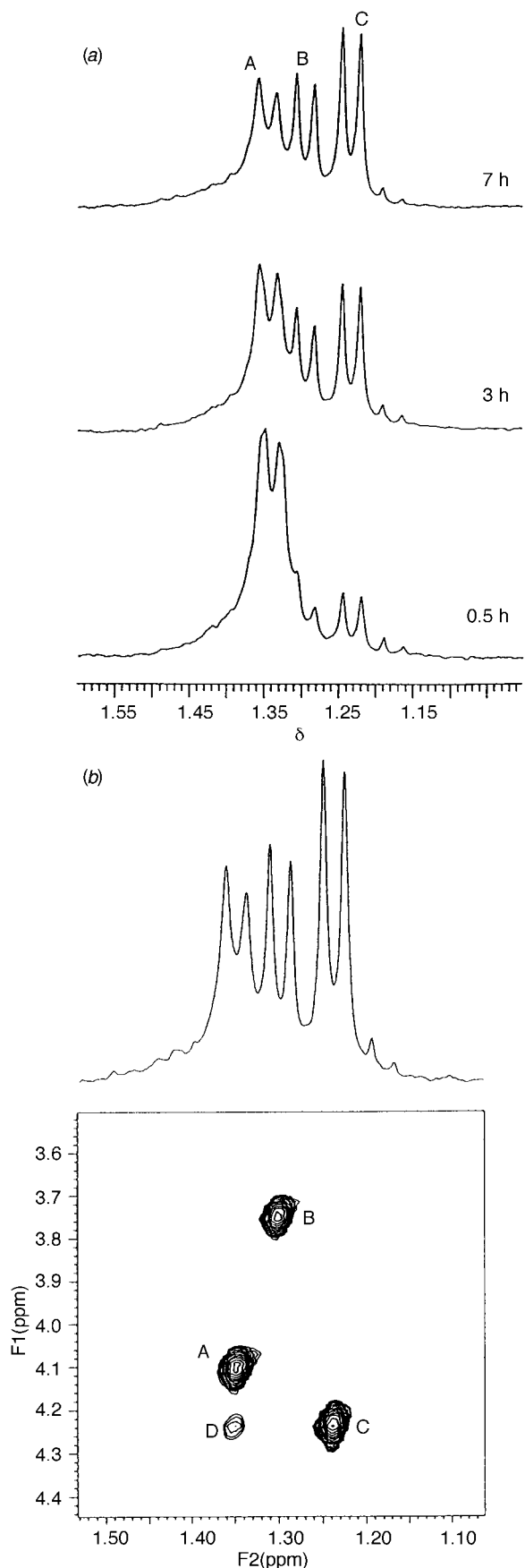


**Fig. 8** (a) One-dimensional  $^1\text{H}$  NMR spectra of the  $5'\text{-CH}_3$  peaks (DX and 13 mol equivalents of  $\text{SnCl}_4 \cdot 5\text{H}_2\text{O}$ ) at different times after mixing the reactants (A is the initial reaction product; B and C are intermediate products of the time-dependent reaction).  $[\text{DX}] = 3.8 \times 10^{-3} \text{ M}$ ;  $R = 13$ ; (b)  $5'\text{-H}$ – $5'\text{-CH}_3$  cross-peaks in the two-dimensional  $^1\text{H}$  NMR TOCSY spectrum of the same sample 20 h after preparation (D is an additional reaction product not detected in the one-dimensional spectrum)

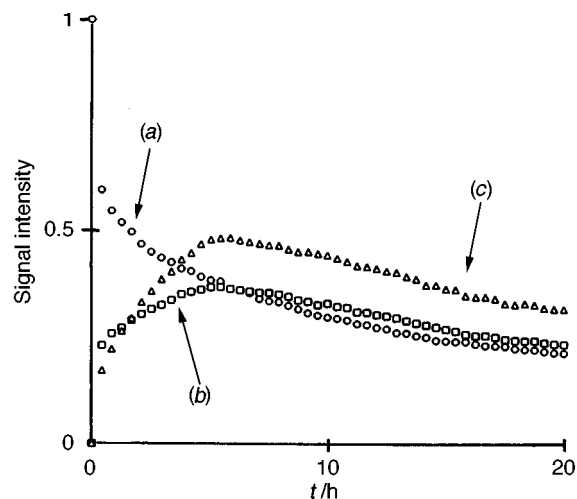
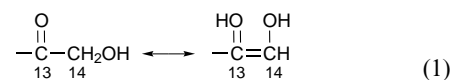


**Fig. 9** Plot of the time dependence of the normalized intensities of the  $5'\text{-CH}_3$   $^1\text{H}$  NMR peaks corresponding to products A, B and C from the  $\text{SnCl}_4\text{-DX}$  (13:1) reaction (see Fig. 8)

$[\text{H}_7]\text{dmf}$ . The one- and two-dimensional  $^1\text{H}$  NMR spectra of the ligand alone were well resolved and the spectral pattern resembled that of the DX daunosamine moiety. On addition of  $\text{Sn}^{\text{IV}}$  only one new species was detected in contrast to the reaction of DX, although the chemical shift changes were similar. Using the same labelling as for DX for clarity, the  $3'\text{-H}$  resonance shifted from  $\delta$  3.66 to 3.80, and also in this case a new peak appeared at  $\delta$  8.44 and was assigned, *via* a two-dimensional TOCSY experiment, to the  $3'\text{-NH}_2$  protons of methyl- $\beta$ -L-daunosamine. For DA, as for DX, it was not possible to assign peaks to  $4'\text{-H}$ , due to spectral overlap. The CD and electronic absorption spectral data on  $\text{Sn}^{\text{IV}}\text{-DX}$  systems indicate that metal binding does not involve deprotonation of the phenolic groups and the results of the experiments with modified anthracyclines (Table 4) imply that the side chain at  $\text{C}^9$  is essential for the metal–drug interaction, thus suggesting that metal binding may occur at this site. The  $^1\text{H}$  NMR findings, and in particular the disappearance of the  $14\text{-CH}_2$  resonance upon interaction of DX with  $\text{Sn}^{\text{IV}}$ , not only support the conclusions of the other spectroscopies, but also suggest that binding to the  $\text{C}^9$  side chain could involve an enolization mechanism, shown in reaction (1), which would allow the formation of a five-



membered chelate ring. Such keto–enol tautomerization of the  $\alpha$ -ketol side chain has been proposed as the first step in the degradation reaction of the drug in water.<sup>36</sup> Unfortunately it was not possible to assign readily the expected singlet for 14-H in the tautomer which may be overlapped in the  $\delta$  7.5–9 region.

The shifts of the  $8\text{-H}_{\text{a,b}}$  and  $10\text{-H}_{\text{a,b}}$  signals in the  $^1\text{H}$  NMR spectrum of the complex relative to the free ligand might be due to a change in the chair conformation of the A ring,<sup>31,33</sup> accompanying enolization of the side chain and binding. The one- and two-dimensional  $^1\text{H}$  NMR spectra, with progressive changes to the  $5'\text{-H}$  and  $5'\text{-CH}_3$  resonances (Figs. 8 and 9), also provide evidence for interactions of  $\text{Sn}^{\text{IV}}$  with the daunosamine moiety of DX.

It has been reported that the interaction of  $\text{PdCl}_2$  or  $\text{PtCl}_2$  with DX in dmf involves binding of the metal to the  $3'\text{-amino}$  group of the free base drug, with no reaction at the chromophore.<sup>39</sup> The shifts we observe for the  $2'\text{-H}$  and  $3'\text{-H}$  signals, as well as the changes exhibited by the  $5'\text{-CH}_3$  and  $5'\text{-H}$  resonances, may be attributable to N–O chelation by  $\text{Sn}^{\text{IV}}$  with deprotonation of  $4'\text{-OH}$ , as suggested by Allman and Lenkinski<sup>39</sup> for  $\text{Pt}^{\text{II}}$  and  $\text{Pd}^{\text{II}}$ .

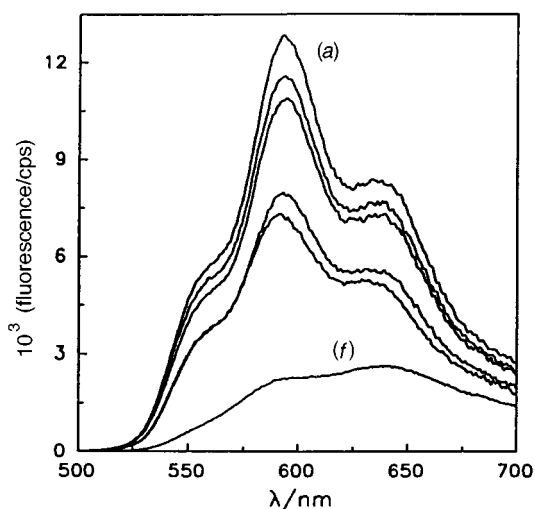


**Fig. 10** Fluorescence spectra of the  $\text{Sn}^{\text{IV}}$ -DX system in dmf at different values of  $R$ , the metal-to-ligand mol ratio. (a) to (f)  $R = 0, 0.5, 1.0, 1.5, 2.0, 68$ , respectively.  $[\text{DX}] = 7.8 \times 10^{-5}$  M. Excitation wavelength 460 nm. Each spectrum was acquired 20 h after the preparation of the sample

It is, however, necessary to underline at this point that the systems investigated by NMR spectroscopy are at different concentrations compared to those used for optical spectroscopy and therefore the kinetic events in the two systems will differ. It is reasonable to assume that the initial product A seen by  $^1\text{H}$  NMR spectroscopy after a few minutes is the one present at completion of the first reactive step (after several hours) at the lower concentrations used for optical spectroscopy. The progressive appearance of several species (labelled B, C and D) seen by  $^1\text{H}$  NMR spectroscopy would correspond to the evolution of the tin-DX system towards more complicated equilibria involving several different species, and the loss of the isosbestic points for the first step in the electronic absorption spectrum. The rate of attainment of the first step increases, and its duration decreases with  $R$  and with the concentration of the reactants.

A careful consideration of the above results is needed to propose reasonable models for  $\text{Sn}^{\text{IV}}$ -DX complexes. Doxorubicin has a characteristic fluorescence spectrum in dmf with maxima at 590 and 640 nm, and a shoulder at 550 nm, with excitation wavelength 460 nm, and a strong quenching of fluorescence is observed upon interaction with tin, increasing with the value of  $R$  and eventually leading to complete disappearance of the spectrum (Fig. 10). Similar effects have been reported when autoassociation phenomena of the drug occur.<sup>30</sup> The CD spectrum of DX, on the other hand, exhibits as the main change due to interaction with tin, a shift of the negative band at 290 nm to longer wavelength as  $R$  increases, reaching 310 nm for  $R \geq 50$ . Such a shift, which is not observed for complexes with other metal cations or following dimerization, has instead been reported for doxorubicin gels, for which the proposed structure is a supra-molecular aggregate with the doxorubicin molecules stacked helically.<sup>40</sup> These observations, together with the low resolution of the electronic absorption spectrum (Fig. 1), suggest that DX molecules aggregate in solution with some degree of stacking. The NMR results, on the other hand, clearly establish that tin binds at two sites on the DX molecule. Therefore the aggregates may involve stacking of drug molecules bound to the metal either through the  $\text{C}^9$  side chain or through the daunosamine ring. Interaction of  $\text{Sn}^{\text{IV}}$  with doxorubicin in dmf thus seems to imply enolization of the  $\alpha$ -ketol side chain and deprotonation of the 3'-amino group prior to complex formation, which might occur either by binding at the 3' and 4' positions of the sugar moiety or at the 13 and 14 positions of the aglycone.

## Experimental

### Chemicals

The compound  $\text{SnCl}_4 \cdot 5\text{H}_2\text{O}$  was a RPE product obtained from Carlo Erba and used without purification; dmf was a Fluka purissimum *p.a.* product and was degassed with ultra-high purity  $\text{N}_2$  gas for at least 5 h before use. Doxorubicin was the kind gift of Farmitalia-Carlo Erba and was used as received. Methyl- $\beta$ -L-daunosaminide hydrochloride was purchased from Sigma, and heptadeutero- $N,N$ -dimethylformamide from Aldrich and was carefully degassed with  $\text{N}_2$  before use. Some of the CD measurements were made using a clinical preparation of DX, Adriblastine by Pharmacia s.a. All the other anthracyclines and model compounds were obtained from Rhône Poulenc.

### Instrumentation

A Varian Cary 1E instrument, interfaced with an IBM 450DX 2/S data system was used for electronic spectra acquisition and processing together with quartz Suprasil cuvettes (Hellma). The circular dichroism spectra were recorded with a Jobin-Yvon Mark V Dichrograph and fluorescence spectra with a SPEX Fluorolog 2 instrument by SPEX Industries Inc. (excitation wavelength 460 nm, pathlength  $3 \times 3$  mm). Optical and NMR spectra were collected at 25 °C. The NMR spectra were recorded on the following instruments: JEOL GSX500 ( $^1\text{H}$  500.63 MHz), Bruker DRX500 ( $^1\text{H}$  500.13 MHz), Bruker AMX400 ( $^1\text{H}$  400.13 MHz) and JEOL GSX270 ( $^1\text{H}$  270.17 MHz,  $^{119}\text{Sn}$  100.73 MHz), using 5 mm tubes for  $^1\text{H}$  and 10 mm tubes for  $^{119}\text{Sn}$  experiments.

Typical acquisition parameters for  $^1\text{H}$  NMR one-dimensional spectra were 45–60° pulses, 32 K points, 128–512 scans, 2.5 s acquisition time and 2.7 s pulse delay. Proton NMR two-dimensional TOCSY experiments used similar experimental conditions, with 8–16 scans and 65 ms mixing time, with acquisition of 2048 data points in the F1 dimension and 512 data points in the F2 dimension. The residual water peak was suppressed with homogated secondary irradiation when necessary, e.g. for samples containing  $\text{SnCl}_4 \cdot 5\text{H}_2\text{O}$  in excess. Tin-119 NMR spectra were acquired with 32 K points, 2.6 s acquisition time and 2.5 s pulse delay with gated proton decoupling to avoid the effect of the negative NOE of  $^{119}\text{Sn}$ . The chemical shift references were the downfield  $^1\text{H}$  methyl peak of dmf ( $\delta$  3.001 relative to  $\text{SiMe}_4$ ), and external 80 mm dimethyltin aqua ion  $[\text{Me}_2\text{Sn}(\text{H}_2\text{O})_4]^{2+}$  at pH 1.3 for the  $^{119}\text{Sn}$  NMR spectra,<sup>41</sup> verified before and after each experiment. Exponential, Gaussian, or sine-bell window functions were applied to the free induction decays prior to transformation as required. The time evolution of the NMR spectra was followed by recording one-dimensional  $^1\text{H}$  NMR spectra every 25 min for 20 h. The intensities of the 5'- $\text{CH}_3$  peaks were normalized to the initial peak intensity and plotted *versus* time.

### Sample preparation

All the samples were prepared at ambient temperature immediately before use. The DX solutions were always prepared in the dark and under nitrogen flux to minimize degradation of the drug by oxygen and light. For electronic absorption spectroscopy, both DX and  $\text{SnCl}_4 \cdot 5\text{H}_2\text{O}$  were dissolved in carefully degassed dmf at concentrations twice those required. Equal amounts of the two solutions were then introduced into the two compartments of a tandem cell (optical pathlength  $2 \times 4.375$  mm) to obtain the initial (zero time) spectrum before mixing for the successive measurements, the mixing time being less than 30 s. The samples for NMR experiments were prepared by adding directly to a 3.8 mm solution of DX in  $[\text{D}_2\text{H}_5]\text{dmf}$  in the NMR tube 1, 2 or 13 mol equivalents of  $\text{SnCl}_4 \cdot 5\text{H}_2\text{O}$ , either from a concentrated solution of the compound in  $[\text{D}_2\text{H}_5]\text{dmf}$  or as a solid. A 13 mm  $[\text{D}_2\text{H}_5]\text{dmf}$  solution of methyl- $\beta$ -L-

daunosaminide hydrochloride was prepared immediately before use and 1 or 13 mol equivalents of  $\text{SnCl}_4 \cdot 5\text{H}_2\text{O}$  were added directly to the NMR tube.

## Acknowledgements

We thank Professor Arlette Garnier-Suillerot for her kind hospitality to one of us (E. B.) at the Université de Paris Nord and for the many stimulating discussions and Professor PierLuigi Luisi for access to a fluorescence spectrometer at ETH in Zürich. We thank the University of London Intercollegiate Research Service Biomedical NMR Centre at Birkbeck College, Biotechnology and Biological Sciences Research Council and Medical Research Council for provision of facilities. The financial support of EC (Contract ERBCHRCT 940589), of the Italian Ministero dell'Università e della Ricerca Scientifica e Tecnologica and of Italian National Council of Research (grants 93.03020.CT03 and 94.01555.CT03) is gratefully acknowledged.

## References

- 1 J. W. Lown (Editor), *Anthracycline and anthracenedione-based anticancer agents*, Elsevier, Amsterdam, 1988, vol. 6.
- 2 S. T. Crooke and S. D. Reich, (Editors), *Anthracyclines: current status and new developments*, Academic Press, New York, 1980.
- 3 A. U. Buzdar, C. Marcus, T. L. Smith and G. R. Blumenschein, *Cancer*, 1985, **55**, 2761 and refs. therein.
- 4 L. J. Steinherz, P. G. Steinherz, C. T. C. Tahn, G. Heller and M. L. Murphy, *J. Am. Med. Assoc.*, 1991, **266**, 1672 and refs. therein.
- 5 F. Villani, E. Monti, L. Favalli, E. Lanza and P. Poggi, *IRCS Med. Sci.*, 1986, **14**, 282.
- 6 P. A. J. Speth, Q. G. C. M. van Hoesel and C. Haanen, *Clin. Pharmacokinet.*, 1988, **15**, 15.
- 7 A. Garnier-Suillerot, ref. 1, ch. IV, pp. 129–161 and refs. therein.
- 8 M. M. L. Fiallo and A. Garnier-Suillerot, *Biochemistry*, 1986, **25**, 924.
- 9 F. Zunino, G. Savi and A. Pasani, *Cancer Chemother. Pharmacol.*, 1986, **18**, 180.
- 10 P. K. Dutta and J. A. Hutt, *Biochemistry*, 1986, **25**, 691.
- 11 R. E. Lenkinski and S. Sierke, *J. Inorg. Biochem.*, 1985, **24**, 59.
- 12 D. Gelvan, E. Berg, P. Saltman and A. Samuni, *Biochem. Pharmacol.*, 1990, **39**, 1289.
- 13 I. J. McLennan and R. E. Lenkinski, *J. Am. Chem. Soc.*, 1984, **106**, 6905.
- 14 T. Yotsuyanagy, N. Ohta, N. Tanaka and K. Ikeda, *Chem. Pharm. Bull.*, 1990, **38**, 3102.
- 15 H. Beraldo, A. Garnier-Suillerot, L. Tosi and F. Lavelle, *Biochemistry*, 1985, **24**, 284.
- 16 F. Capolongo, M. Giomini, A. M. Giuliani, B. F. Matzanke, U. Russo, A. Silvestri, A. X. Trautwein and R. Barbieri, *J. Inorg. Biochem.*, 1997, **65**, 115.
- 17 H. B. Haj-Tayeb, M. M. L. Fiallo, A. Garnier-Suillerot, T. Kiss and H. Kozłowski, *J. Chem. Soc., Dalton Trans.*, 1994, 3689.
- 18 E. Pereira, M. M. L. Fiallo, A. Garnier-Suillerot, T. Kiss and H. Kozłowski, *J. Chem. Soc., Dalton Trans.*, 1993, 455.
- 19 R. G. Canada and R. G. Carpentier, *Biochim. Biophys. Acta*, 1991, **1073**, 136.
- 20 G. Bonadonna, *Advances in anthracycline chemotherapy: epirubicin*, Masson Italia, Milano, 1984.
- 21 F. Arcamone, *Cancer Res.*, 1985, **45**, 5995.
- 22 W. Priebe *ACS Symp. Ser.*, 1995, **574**.
- 23 H. Beraldo, A. Garnier-Suillerot and L. Tosi, *Inorg. Chem.*, 1983, **22**, 4117.
- 24 J. J. Zuckermann (Editor), *Tin and malignant cell growth*, CRC Press, Boca Raton, FL, 1988.
- 25 M. Gielen, *NATO ASI Ser. H*, 1990, **37**.
- 26 R. L. Mills, C. W. Walter, L. Venkataraman, K. Pang and J. J. Farrell, *Nature*, 1988, **336**, 787.
- 27 W. M. Reiff, R. L. Mills and J. J. Farrell, *Hyperfine Interact.*, 1990, **58**, 2525.
- 28 J. W. Lown (Editor), ref. 1, chs. VII, X and XIV.
- 29 N. Henry, E. O. Fantine, J. Bolard and A. Garnier-Suillerot, *Biochemistry*, 1985, **24**, 7085.
- 30 S. R. Martin, *Biopolymers*, 1980, **19**, 713.
- 31 T. Allman and R. E. Lenkinski, *Can. J. Chem.*, 1987, **65**, 2405.
- 32 I. J. McLennan, R. E. Lenkinski and Y. Yanuka, *Can. J. Chem.*, 1985, **63**, 1233.
- 33 R. Mondelli, E. Ragg, G. Fronza and A. Arnone, *J. Chem. Soc., Perkin Trans. 2*, 1987, 15.
- 34 F. J. C. Rossotti and H. Rossotti, *The determination of stability constants*, McGraw-Hill, New York, 1961, pp. 47–51.
- 35 M. Menozzi, L. Valentini, E. Vannini and F. Arcamone, *J. Pharm. Sci.*, 1984, **73**, 766.
- 36 J. H. Beijnen, O. A. G. J. van der Houwen and W. J. M. Underberg, *Int. J. Pharm.*, 1986, **32**, 123.
- 37 J. Bouma, J. H. Beijnen, A. Bult and W. J. M. Underberg, *Pharm. Weekbl. Sci. Ed.*, 1986, **8**, 109.
- 38 M. M. L. Fiallo, H. Tajeb-Bel Haj and A. Garnier-Suillerot, *Metal Based Drugs*, 1994, **1**, 183.
- 39 T. Allman and R. E. Lenkinski, *J. Inorg. Biochem.*, 1987, **30**, 35.
- 40 M. Giomini, A. M. Giuliani, M. Giustini and E. Trotta, *Biophys. Chem.*, 1992, **45**, 31.
- 41 V. Cucinotta, A. Gianguzza, G. Maccarrone, L. Pellerito, R. Purrello and E. Rizzarelli, *J. Chem. Soc., Dalton Trans.*, 1992, 2299.

Received 15th April 1997; Paper 7/02588B